Reprinted from October 1985, Vol. 107, Journal of Vibration, Stress, and Reliability in Design

# A Conical Beam Finite Element for Rotor Dynamics Analysis

**L. M. Greenhill**
Garrett Turbine Engine Company,
Phoenix, AZ

**W. B. Bickford**

**H. D. Nelson**
Mechanical and Aerospace Engineering,
Arizona State University,
Tempe, AZ 85287

*The development of finite element formulations for use in rotor dynamics analysis has been the subject of many recent publications. These works have included the effects of rotatory inertia, gyroscopic moments, axial load, internal damping, and shear deformation. However, for most closed-form solutions, the element geometry has been limited to a cylindrical cross-section. This paper extends these previous works by developing a closed-form expression including all of the above effects in a linearly tapered conical cross-section element. Results are also given comparing the formulation to previously published examples, to stepped cylinder representations of conical geometry, and to a general purpose finite element elasticity solution. The elimination of numerical integration in the generation of the element matrices, and the ability of the element to represent both conical and cylindrical geometries, make this formulation particularly suited for use in rotor dynamic analysis computer programs.*

## Introduction

Over the last several years, many investigators have extended the capability of rotor dynamics analysis using finite elements. Early formulations, such as Nelson and McVaugh [1], developed a Rayleigh beam theory finite rotating shaft element which included the effects of translational and rotatory inertia, gyroscopic moments, and axial load. This development was subsequently generalized by Zorzi and Nelson [2] to include the effects of internal viscous and hysteretic damping. Later, Nelson [3] added shear deformation to the Rayleigh beam theory to develop a Timoshenko beam element, which was then extended by Ozguven and Ozkan [4] to include the internal damping model of Zorzi and Nelson. All of these formulations considered the axial cross-section of the element to be cylindrical, which allows area and inertia to be considered constant with respect to length. The motion of these elements was represented by eight degrees of freedom: two translations and two rotations at the element ends.

Modern rotor systems utilize geometry which is usually far from being uniform as a function of length. These cross-sectional changes are mainly accommodated by modeling the rotor as a collection of stepped cylinders. For conical cross-sections, the errors introduced by the stepped cylinder approach may be quite large.

As a result, Rouch and Kao [5], developed a linearly tapered Timoshenko beam element for use in rotor dynamics. This element was based upon the work of Thomas, Wilson, and Wilson [6], who determined that the most optimum representation of the shear deformation was to add two additional coordinates at each element end, resulting in twelve degrees of freedom per element. The Rouch and Kao element extended the earlier formulation by including gyroscopic effects and representing the area and inertia as second and fourth order polynomials as a function of radius. The element matrices were obtained by numerical integration, and as such, no closed form expressions were presented. It was also indicated that the additional shear deformation coordinates could be condensed out of the element or system equations without significant loss of accuracy. Later, To [7] developed closed form polynomial mass and stiffness expressions for a linearly tapered Timoshenko element, again using the twelve degree of freedom representation of Thomas, Wilson, and Wilson.

This paper extends the linearly tapered Timoshenko beam theory element by using the kinematic representation of Thomas, Wilson, and Wilson to develop closed form polynomial expressions for element matrices suitable for use in finite element rotor dynamics computer programs. The element includes the effects of translational and rotatory inertia, gyroscopic moments, axial load, internal viscous and hysteretic damping, and mass center eccentricity. System equations of motion are also presented in both fixed and rotating reference frames. Numerical examples are given comparing the use of the conical element to a previously published test case, to stepped cylinder representations, and to a general purpose finite element elasticity solution.

## Coordinates and Shape Functions

A typical axial cross-section of a linearly tapered finite element is shown in Fig. 1. Each end of the element is associated with an inner and outer radius, denoted by $r$ and $R$, with the subscripts $i$ and $j$ referring to the left ($s=0$) and right ($s=l$) ends of the element, respectively. Defining a non-dimensional position coordinate $\xi$, equal to the ratio $s/l$, the inner and outer radii may be expressed as

Contributed by the Technical Committee on Vibration and Sound and presented at the Design Engineering Technical Conference, Cincinnati, Ohio, September 10-13, 1985, of THE AMERICAN SOCIETY OF MECHANICAL ENGINEERS. Manuscript received at ASME Headquarters, June 11, 1985. Paper No. 85-DET-32.

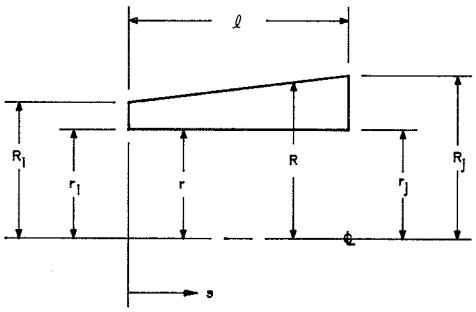


Fig. 1 Conical element axial cross section geometry

$$r = r_i(1-\xi)+r_j\xi \quad (1(a))$$

$$R = R_i(1-\xi)+R_j\xi \quad (1(b))$$

Representing the ratios of inner and outer radii on each end as $\rho$ and $\sigma$, which are equal to $r_j/r_i$ and $R_j/R_i$ respectively, allows equations (1) to be rewritten

$$r = r_i(1+(\rho-1)\xi) \quad (2(a))$$

$$R = R_i(1+(\sigma-1)\xi) \quad (2(b))$$

Using equations (2) in a cross-sectional area equation results in the following second order polynomial expression

$$A=\pi(R^2-r^2)=A_i[1+\alpha_1\xi+\alpha_2\xi^2] \quad (3)$$

where the coefficients are

$$A_i = \pi(R_i^2-r_i^2)$$

$$\alpha_1 = 2[R_i^2(\sigma-1)-r_i^2(\rho-1)]/(R_i^2-r_i^2)$$

$$\alpha_2 = [R_i^2(\sigma-1)^2-r_i^2(\rho-1)^2]/(R_i^2-r_i^2)$$

Similarly for cross-sectional inertia, the use of equations (2) results in a fourth order polynomial expression of

$$I=\pi(R^4-r^4)/4=I_i[1+\delta_1\xi+\delta_2\xi^2+\delta_3\xi^3+\delta_4\xi^4] \quad (4)$$

where the coefficients are

$$I_i = \pi(R_i^4-r_i^4)/4$$

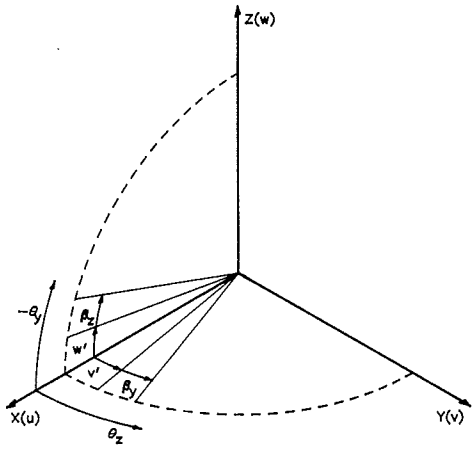


Fig. 2 Kinematic relationships between element degrees of freedom

$$\delta_1 = 4[R_i^4(\sigma-1)-r_i^4(\rho-1)]/(R_i^4-r_i^4)$$

$$\delta_2 = 6[R_i^4(\sigma-1)^2-r_i^4(\rho-1)^2]/(R_i^4-r_i^4)$$

$$\delta_3 = 4[R_i^4(\sigma-1)^3-r_i^4(\rho-1)^3]/(R_i^4-r_i^4)$$

$$\delta_4 = [R_i^4(\sigma-1)^4-r_i^4(\rho-1)^4]/(R_i^4-r_i^4)$$

The primary coordinate reference system is illustrated in Fig. 2. The $(XYZ)$ triad is a fixed reference with the $X$-axis coinciding with the undeformed centerline of the element. Although not shown, the $(xyz)$ triad is a rotating reference with the $x$-axis coincident with $X$, and the $y$- and $z$-axes rotating at a uniform rate $\omega$ about the $X$-axis. The element is considered to be initially straight and is modeled with twelve degrees of freedom: two translations, two rotations, and two shear deformations at each end-point of the element. The diametral cross-section of the element is considered to be circular.

The translation of the element, neglecting axial motion, is given by the two displacements $(v,w)$, and the shear defor-

## Nomenclature

$\alpha$ = area polynomial coefficient
$\beta$ = inertia polynomial coefficient
$\rho,\sigma$ = element end inner and outer radii ratio
$\mu$ = mass per unit volume
$\epsilon,\zeta$ = location of mass center
$\Omega$ = spin speed
$\omega$ = whirl speed
$\lambda$ = whirl ratio, $\Omega/\omega$
$\eta_V,\eta_H$ = internal viscous, hysteretic damping coefficient
$[\eta]$ = internal damping matrix
$[\psi]$ = translation dependent rows of shape function matrix
$[\phi]$ = rotation dependent rows of shape function matrix
$[\chi]$ = shear dependent rows of shape function matrix
$\xi$ = ratio of axial position to element length, $s/l$
$\theta$ = rotational displacements
$\beta$ = shear displacements
$s$ = axial position along element
$l$ = length of element
$r,R$ = inner, outer radius of element end
$A$ = element area (function of axial position)
$I$ = element inertia (function of axial position)
$E$ = element elastic modulus (constant)
$E_P$ = potential energy
$E_K$ = kinetic energy
$E_D$ = dissipation function
$G$ = element shear modulus (constant)
$k$ = transverse shear form factor (constant)
$P$ = element axial load (constant)
$t$ = time
$u,v,w$ = translational displacements in $X$, $Y$, and $Z$ directions
$\{p\}$ = element end displacement vector, rotating frame coordinates
$\{q\}$ = element end displacement vector, fixed frame coordinates
$\{Q\}$ = element unbalance force vector
$[K_B]$ = bending stiffness matrix
$[K_S]$ = shear stiffness matrix
$[K_A]$ = axial load stiffness matrix
$[K_C]$ = circulation matrix
$[M_T]$ = translational mass matrix
$[M_R]$ = rotatory mass matrix
$[G]$ = gyroscopic effect matrix
$[N]$ = transformation matrix
$[R]$ = fixed to whirl frame transformation matrix

### Subscripts

$i,j$ = left and right element ends
1,2, . . = particular term in a matrix or polynomial expression

### Superscripts

$'$, $\cdot$ = position, time differentiation

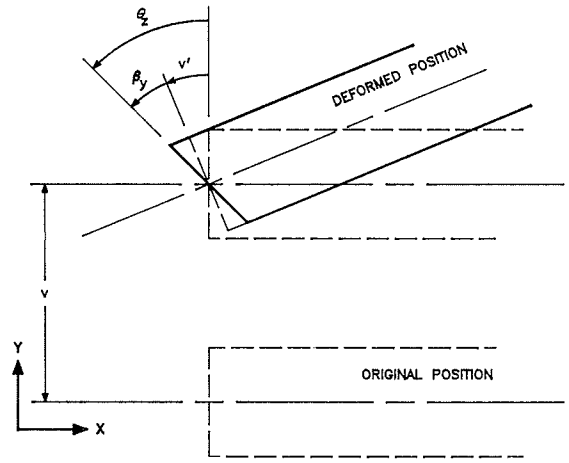


Fig. 3 Deformed element axial cross-section (X-Y plane)

mation contribution is expressed as $(\beta_y,\beta_z)$. The rotation of the cross-section is defined by the relationships

$$\theta_y = -w' - \beta_z \quad (5(a))$$

$$\theta_z = v' + \beta_y \quad (5(b))$$

as shown in Fig. 2. Note that the sign of $\theta_y$ is set negative in order to obey kinematic constraints. The deformed shape of an element in the $X$-$Y$ plane is shown in Fig. 3, which illustrates the additional rotation of the cross-section due to shear.

The translation of a point internal to the element relative to the end-point displacements is approximated by the relation

$$\begin{Bmatrix} v(s,t) \\ w(s,t) \end{Bmatrix} = [\psi(s)]\{q(t)\} \quad (6)$$

with the components of $[\psi]$ given in the Appendix. The individual shape functions are obtained by assuming the transverse displacement varies cubically as a function of length. Using equations (5) and (6), and assuming the shear deformation varies linearly with length, the rotation of the cross-section is given by the relation

$$\begin{Bmatrix} \theta_y(s,t) \\ \theta_z(s,t) \end{Bmatrix} = [\phi(s)]\{q(t)\} \quad (7)$$

and the deformation of the element due to shear is expressed by

$$\begin{Bmatrix} \beta_y(s,t) \\ \beta_z(s,t) \end{Bmatrix} = [\chi(s)]\{q(t)\} \quad (8)$$

with the components of $[\phi]$ and $[\chi]$ given in the Appendix.

The order of the coordinates in the end-point displacement vector was chosen as

$$\{q\} = \{v_i, w_i, \theta_{yi}, \theta_{zi}, v_j, w_j, \theta_{yj}, \theta_{zj}, \beta_{yi}, \beta_{zi}, \beta_{yj}, \beta_{zj}\}^T \quad (9)$$

in which the first eight terms are identical to those in [1–4], and the last four are the shear deformation contributions. The order of coordinates in equation (9) was selected to facilitate condensation of the shear deformation coordinates.

## Element Equations

The element equations can be derived through the use of Lagrange's equations. As such, quadratic expressions for potential energy, kinetic energy, dissipative functions, and generalized forces are required, and will be developed in separate sections below.

**Potential Energy.** Using Timoshenko beam theory, the differential potential energy can initially be written as a combination of elastic bending, shear, and axial load expressions, with the effects of internal damping on bending strain energy to be included separately. In terms of the element internal degrees of freedom, the potential energy is

$$2dE_P = EI(\theta_y'^2 + \theta_z'^2)ds + kGA(\beta_y^2 + \beta_z^2)ds + P(v'^2 + w'^2)ds \quad (10)$$

Equation (10) may be integrated over the length of the element to obtain an expression for potential energy in terms of three discrete stiffness matrices as

$$2E_P = \{q\}^T([K_B] + [K_S] + [K_A])\{q\} \quad (11)$$

in which $[K_B]$ is the bending stiffness matrix, $[K_S]$ the shear stiffness matrix, and $[K_A]$ the axial stiffness matrix. The individual matrices are obtained from equations (6, 7, 8) as

$$[K_B] = \int_0^l EI(\xi)[\phi']^T[\phi']ds \quad (12(a))$$

$$[K_s] = \int_0^l kGA(\xi)[\chi]^T[\chi]ds \quad (12(b))$$

$$[K_A] = \int_0^l P[\psi']^T[\psi']ds \quad (12(c))$$

The components of each of the three stiffness matrices, equations (12), are given in the Appendix. Each term in the bending and shear stiffness matrices, $[K_B]$ and $[K_S]$, are fourth and second order polynomials, respectively, due to the variation of inertia and area with length, equations (3) and (4). Axial load is assumed constant as a function of length, thus each term in the axial stiffness matrix is a single value of order zero.

**Kinetic Energy.** The kinetic energy expression is a combination of translational and rotational components. In terms of the element internal degrees of freedom, the differential kinetic energy may be written as

$$2dE_K = \mu A(\dot{v}^2 + \dot{w}^2)ds + I_d(\dot{\theta}_y^2 + \dot{\theta}_z^2)ds + I_p\Omega^2 ds - \Omega I_p\dot{\theta}_z\theta_y ds \quad (13)$$

Equation (13) may be integrated over the length of the element to obtain the complete kinetic energy of the element. In terms of discrete matrices, the energy expression may be represented by the following relation

$$2E_K = \{\dot{q}\}^T([M_T] + [M_R])\{\dot{q}\} + \Omega\{q\}^T[G]\{q\} \quad (14)$$

in which $[M_T]$ is the translational mass matrix, $[M_R]$ the rotatory mass matrix, and $[G]$ the gyroscopic matrix. The individual matrices are defined for the purpose of forming the Lagrangian, and are obtained from equations (6, 7, 8) as

$$[M_T] = \int_0^l \mu A(\xi)[\dot{\psi}]^T[\dot{\psi}]ds \quad (15(a))$$

$$[M_R] = \int_0^l \mu I(\xi)[\dot{\phi}]^T[\dot{\phi}]ds \quad (15(b))$$

$$[G] = \int_0^l 2\mu I(\xi)[\dot{\phi}]^T[N][\dot{\phi}]ds \quad (15(c))$$

with $I_d = \mu I(\xi)$, $I_p = 2\mu I(\xi)$, and $[N]$ a $2\times 2$ skew symmetric transformation matrix as defined in the Appendix. The components of each of the matrices in equation (15) are also given in the Appendix. Each term is a second or fourth order polynomial.

**Internal Damping – Bending Potential Energy and Dissipation Function.** The incorporation of internal damping uses the same type of linear models as [2]. Proceeding from the constitutive relationship between axial stress to axial strain, the differential bending energy and dissipation functions for the Timoshenko element with internal damping are defined as

$$2dE_P = EI(\xi)\{q\}^T[\phi']^T\{[\eta][\phi'] + \eta_V[N]^T[\phi']\}\{q\}ds \quad (16(a))$$

$$2dE_D = \eta_V EI(\xi)\{\dot{q}\}^T[\phi']^T[\phi']\{\dot{q}\}ds \quad (16(b))$$

with the components of $[\eta]$ given in the Appendix. These expressions differ from those presented in [2] due to the relationship between bending and shear as given by equations (5).

Equation (16($a$)) may be expanded and rewritten as

$$2dE_P = EI(\xi)\frac{\eta_H+1}{\sqrt{1+\eta_H{}^2}}\{q\}^T[\phi']^T[\phi']\{q\}ds + EI(\xi)\left\{\frac{\eta_H}{\sqrt{1+\eta_H{}^2}} + \Omega\eta_V\right\}\{q\}^T[\phi']^T[N]^T[\phi']\{q\}ds$$

and then may be integrated along with equation (16($b$)) over the length of the element to form matrix expressions for the bending potential energy and dissipation functions as

$$2E_P = \frac{\eta_H+1}{\sqrt{1+\eta_H{}^2}}\{q\}^T[K_B]\{q\} + \left\{\frac{\eta_H}{\sqrt{1+\eta_H{}^2}} + \Omega\eta_V\right\}\{q\}^T[K_C]\{q\} \quad (17(a))$$

$$2E_D = \eta_V\{\dot{q}\}^T[K_B]\{\dot{q}\} \quad (17(b))$$

in which $[K_C]$ is the internal damping circulation matrix, obtained from equations (6, 7, 8) as

$$[K_C] = \int_0^l EI(\xi)[\phi']^T[N]^T[\phi']ds \quad (18)$$

which is skew symmetric and each term is a fourth order polynomial. The components of $[K_c]$ are given in the Appendix. In equations (17), the matrix $[K_B]$ is the bending stiffness matrix given in equation (12($a$)). Thus the incorporation of internal damping results in additional terms in the potential energy expression as well as the creation of a dissipative function. Note that if $[\phi'] = [N]\,[\psi'']$ as in [2], the equations (16) could be transformed to the same expression for bending energy and dissipation functions as contained in [2].

**Generalized Forces.** The only generalized force included in this element formulation is due to distributed unbalance force. For an element with mass center eccentricity ($\epsilon(s)$, $\zeta(s)$), the equivalent unbalance force is represented by

$$\{Q_F\} = \{Q_C\}\cos\Omega t + \{Q_S\}\sin\Omega t \quad (19)$$

in which the force components are

$$\{Q_C\} = \Omega^2\int_0^l \mu A(\xi)[\psi]^T \begin{Bmatrix} \epsilon(s) \\ \zeta(s) \end{Bmatrix} ds \quad (20(a))$$

$$\{Q_S\} = \Omega^2\int_0^l \mu A(\xi)[\psi]^T \begin{Bmatrix} -\zeta(s) \\ \epsilon(s) \end{Bmatrix} ds \quad (20(b))$$

using a linear distribution for mass unbalance over the element as

$$\epsilon(s) = \epsilon_i(1-\xi) + \epsilon_j\xi \quad (21(a))$$

$$\zeta(s) = \zeta_i(1-\xi) + \zeta_j\xi \quad (21(b))$$

the equivalent unbalance force may be obtained from equation (19) by using equations (21) in the integral expressions (20). The unbalance force vector components $\{Q_C\}$ and $\{Q_S\}$ are given in the Appendix.

It can be shown that the element matrices given in equations (12), (15), and (20) are equivalent to the same expressions given in [3] by assuming a uniform cylindrical geometry and reducing the matrices from a size of 12 × 12 to 8 × 8 through static condensation.

## System Equations

In the fixed reference frame ($XYZ$), the system equation of motion may be assembled by the use of Lagrange's equations from the expressions developed in equations (11), (14), (17), and (19). The resulting equation is of the form

$$([M_T]+[M_R])\{\ddot{q}\} + (\eta_V[K_B] - \Omega[G])\{\dot{q}\} + \left\{\frac{\eta_H+1}{\sqrt{1+\eta_H{}^2}}[K_B] + [K_A] + \left(\eta_V\Omega + \frac{\eta_H}{\sqrt{1+\eta_H{}^2}}\right)[K_C]\right\}\{q\} = \{Q_F\} \quad (22)$$

All the matrices contained in equation (22) are symmetric except for the gyroscopic matrix $[G]$ and the circulation matrix $[K_C]$.

For isotropic systems, it is convenient to use the rotating reference frame ($xyz$). The transformation between fixed and rotating frame coordinates is given by

$$\{q\} = [R]\{p\} \quad (23)$$

where $[R]$ is a transformation matrix whose components are given in the Appendix. Use of the transformation equation (23) in the fixed frame equation of motion (22), premultiplying by $[R]^T$, and defining a whirl ratio ($\lambda = \Omega/\omega$), gives the rotating or whirl frame equation of motion as

$$([M_T]+[M_R])\{\ddot{p}\} + \{\eta_V[K_B] + \omega([\hat{M}_T] + (1-\lambda)[G]\}\{\dot{p}\} + \left\{\frac{1}{\sqrt{1+\eta_H{}^2}}\{(1+\eta_H)[K_B] + \eta_H[K_C]\} + [K_A] + \omega\eta_V(\lambda-1)[K_C] - \omega^2([M_T] + (1-2\lambda)[M_R])\right\}\{p\} = \{Q_C\} \quad (24)$$

in which the skew symmetric matrix $[\hat{M}_T]$ is given by the expression

$$[\hat{M}_T] = 2\int_0^l \mu A(\xi)[\psi]^T[N][\psi]ds \quad (25)$$

and the unbalance force vector $\{Q_C\}$ is given by equation (20($a$)).

For a rotor composed of elements formulated in terms of fixed reference coordinates by using equation (22) or in terms of a whirl reference system through the use of equation (24), the system will be composed of an assemblage of individual element matrices, each with size 12×12. This size may be retained throughout the computation, or may be reduced using a static condensation algorithm as outlined in [1], at either the element or system level.

In this study, the elemental reduction approach was used, and each 12×12 element matrix was reduced to an equivalent 8×8 prior to assembly into the global system matrices. This technique was evaluated in [5] and found to result in no significant loss of accuracy. Computationally, this approach is identical to that used for subelement condensation in [1], and as such, the conical element may be treated with the same reduction algorithm. The condensation of element matrices prior to assembly in the global system matrices also facilitates the addition of discrete support connections and lumped masses.

The calculation of whirl speeds or unbalance response uses the same techniques as outlined in [1], and as such, will not be repeated. The addition of internal damping results in

**Table 1 Natural frequencies (Hz) of tapered chimney [6]**

| Mode | Five Elements | | Ten Elements | | Twenty Elements | |
|---|---|---|---|---|---|---|
| | Thomas | Current | Thomas | Current | Thomas | Current |
| 1 | 0.5097 | 0.5092 | 0.5096 | 0.5092 | 0.5096 | 0.5092 |
| 2 | 2.6937 | 2.7024 | 2.6920 | 2.6928 | 2.6918 | 2.6904 |
| 3 | 6.5411 | 6.6725 | 6.5090 | 6.5454 | 6.5072 | 6.5128 |
| 4 | 11.355 | 11.800 | 11.073 | 11.262 | 11.062 | 11.105 |
| 5 | 17.748 | 17.583 | 16.070 | 16.627 | 16.019 | 16.162 |
| 6 | 24.109 | 33.988 | 21.338 | 22.540 | 21.162 | 21.501 |
| 7 | 38.902 | 41.310 | 26.882 | 28.941 | 26.381 | 27.039 |
| 8 | 40.756 | 46.413 | 32.790 | 35.605 | 31.589 | 32.700 |
| 9 | 45.333 | 49.652 | 38.963 | 42.040 | 36.712 | 38.380 |
| 10 | 49.554 | 51.736 | 40.607 | 43.209 | 40.380 | 41.192 |

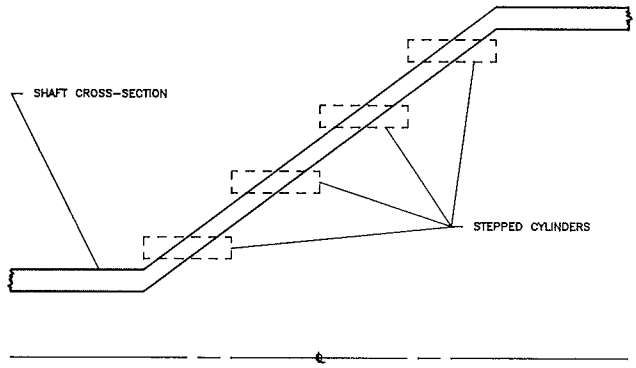


Fig. 4 Typical stepped cylinder representation of conical geometry

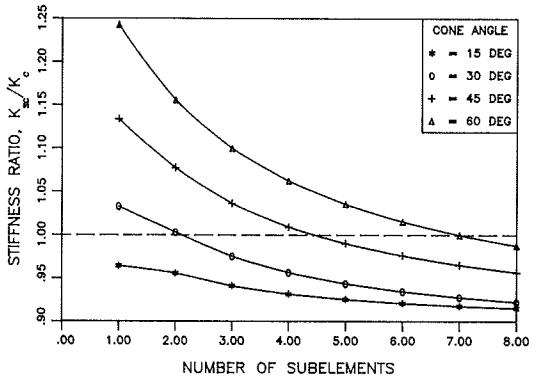


Fig. 5 Single element stepped cylinder versus cone stiffness comparison, term $K_{11}$

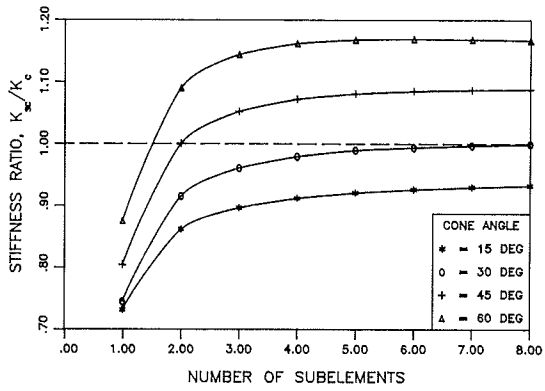


Fig. 6 Single element stepped cylinder versus cone stiffness comparison, term $K_{12}$

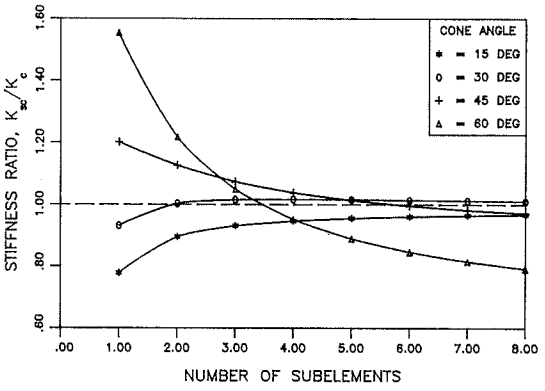


Fig. 7 Single element stepped cylinder versus cone stiffness comparison, term $K_{22}$

parametric terms in the rotating frame whirl speed calculation, which can be accommodated through the use of iteration procedures. In practice, these terms are usually ignored and only undamped natural frequencies are calculated in whirl frame analysis.

## Numerical Examples

Three examples are provided to illustrate the accuracy and use of the conical element. The first is a test case, originally published by Thomas, et al. [6], in which conical elements were used to calculate the natural frequencies of a tapered chimney. Using five, ten, and twenty conical elements, the results from [6] and those obtained from the present formulation are compared in Table 1 for the first ten modes.

As the results indicate, the comparison is quite good, with the present formulation frequencies, in general, slightly higher than those obtained in [6]. It was expected that the frequencies should differ, as the inertia and area representations used in [6] were linear rather than fourth and second order polynomials as in equations (3) and (4). For reference, the frequencies obtained with the present formulation are practically identical to those presented in [5], being consistently larger by a maximum of .35 percent.

The second example compares the use of the conical element with stepped cylinders. As Fig. 4 illustrates, the stepped cylinder representation is used with common rotor dynamics programs to simulate conical structures. For the comparison, the stiffness and natural frequencies were evaluated for a cantilevered cone using from one to eight steps, referred to as subelements as per [1]. Cone angles investigated were 0, 15, 30, 45, and 60 degrees, with the thickness of the cones adjusted for angle, holding the normal thickness to 1.0 cm and the mean radius at the fixed end to 2.0 cm. Table 2 lists the properties of the cones used in this example.

For a single element cantilever cone, fixed at the small end, the stiffness matrix can be reduced to a $2 \times 2$ matrix. The three terms in the resulting matrix may be compared for the stepped cylinder versus conical element formulations. Note that for zero cone angle, the conical element degenerates to a cylindrical formulation as in [3]. In Figs. 5, 6, and 7, the ratio of the stiffness term for the stepped cylinder ($K_{SC}$) to the conical element ($K_C$) is displayed for up to eight subelements. For terms $K_{11}$ and $K_{12}$, translational and translational-rotational

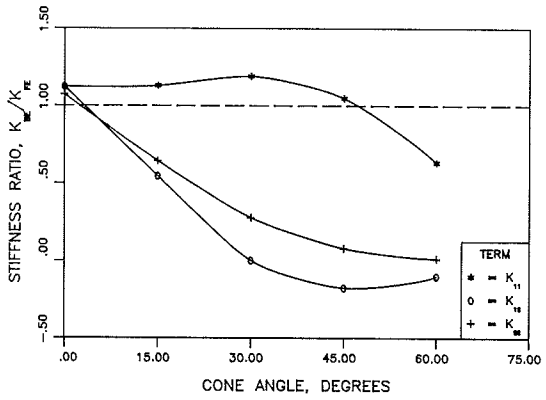


Fig. 8 Single beam element versus finite element elasticity stiffness comparison

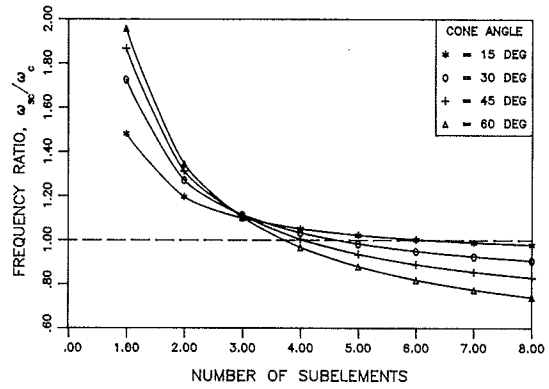


Fig. 9 One element stepped cylinder versus cone frequency comparison, first mode

**Table 2 Conical element test case**

$l = 10.0$ cm $\quad E = 20.0\times10^{10}$ N/m$^2$
$\mu = 8304$ kg/m$^3$ $\quad G = 7.6923\times10^{10}$ N/m$^2$
$k = .900$

| Cone Angle | $R_i$ | $r_i$ | $R_j$ | $r_j$ |
|---|---|---|---|---|
| 0 | 2.500 | 1.500 | 2.500 | 1.500 |
| 15 | 2.518 | 1.482 | 5.197 | 4.161 |
| 30 | 2.577 | 1.423 | 8.351 | 7.197 |
| 45 | 2.707 | 1.293 | 12.707 | 11.293 |
| 60 | 3.000 | 1.000 | 20.321 | 18.321 |

coupling, the comparison results in a family of curves, increasing in value with increasing cone angle. The rotational term $K_{22}$ displays mixed results. In general, the comparison indicates that there is no optimum number of subelements that may be used to represent the conical geometry.

The stiffness terms predicted by the conical element were also compared to those predicted by a general purpose finite element computer code, ANSYS [8]. The basic geometry as given in Table 2 was discretized into 80 axi-symmetric elements. Using cantilever boundary conditions, the resulting displacements were used to calculate an equivalent $2\times2$ single element stiffness matrix. The comparison of the terms in the stiffness matrix is illustrated in Fig. 8 as the ratio of the beam element stiffness term ($K_{BE}$) to that of the finite element ($K_{FE}$).

As the figure indicates, the translational coefficient ($K_{11}$) slightly underestimates the elasticity values. For the cross-coupling ($K_{12}$) and rotatory ($K_{22}$) coefficients, the beam theory significantly overestimates the stiffness as given by the elasticity model, due to the inability of the beam theory to accommodate any ovalizing effects for increasing cone angles. It is somewhat surprising, however, that the deterioration in the agreement between the $K_{12}$ and $K_{22}$ terms is so immediate and rapid with any nonzero cone angle.

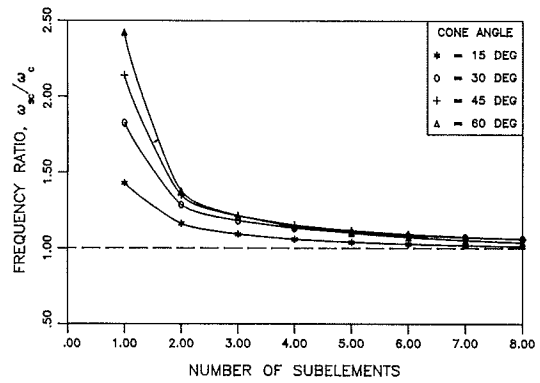


Fig. 10 One element stepped cylinder versus cone frequency comparison, second mode

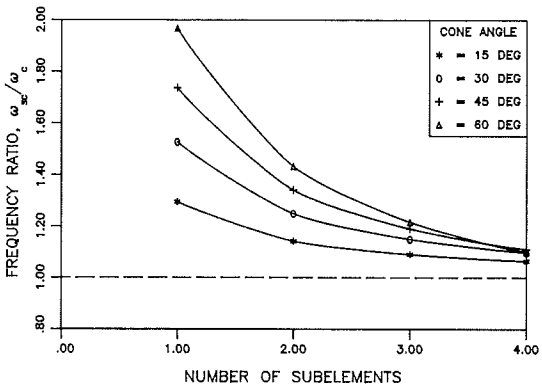


Fig. 11 Two element stepped cylinder versus cone frequency comparison, first mode

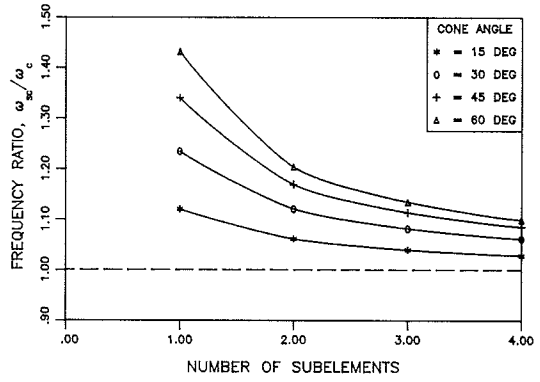


Fig. 12 Two element stepped cylinder versus cone frequency comparison, second mode

An additional comparison, that for natural frequencies of the first two modes, is displayed in Figs. 9–12. In these figures, the ratio of the natural frequency of the cantilevered cone obtained by the use of stepped cylinders ($\omega_{SC}$) to that calculated by the conical element ($\omega_C$) is presented for up to eight subelements. Both one and two elements were used to calculate the frequencies, to illustrate the effect of refinement. As the figures illustrate, the ratio of natural frequencies is poor unless several subelements are used. It is interesting to note that the second mode frequency is always overpredicted using stepped cylinders. The comparison also indicates that no optimum number of stepped cylinders adequately predicts the natural frequencies of both modes for the cone angles surveyed.

## Summary and Conclusions

The equations of motion for a conical beam finite element have been developed from Timoshenko beam theory, and

include the effects of translational and rotational inertia, gyroscopic moments, bending and shear deformation, axial load, and internal damping. Both fixed and rotating frames of reference system equations are presented.

The resulting element formulation was compared to a previously published test case, to stepped cylinder representations, and to a finite element elasticity solution. Good agreement was obtained with the test case. For the stepped cylinders, no optimum number of subelements was found to represent both stiffness and natural frequencies of the cantilever cone example. The elasticity solution disclosed the inability of the beam formulation to account for ovalizing effects for nonzero cone angles.

The conical geometry results in closed-form polynomial expressions for the element matrices. These matrix representations are easily incorporated into finite element rotor dynamics computer programs with minimal increases in computation time and storage requirements. As the element will degenerate to an equivalent cylinder, this formulation can replace rather than add to existing code.

Use of the conical element greatly enhances modeling flexibility. When confronted with conical geometry, the analyst is usually forced to represent the cross-section with a series of stepped cylinders or run independent conical section analyses. Use of the conical element eliminates this process, resulting in a decrease in modeling time and improving the rotor representation.


## Acknowledgment

The authors gratefully acknowledge the programming and computational assistance of Mr. Wen-Jeng Chen in the preparation of this work.


## References


1 Nelson, H. D., and McVaugh, J. M., "The Dynamics of Rotor-Bearing Systems Using Finite Elements," ASME *Journal of Engineering for Industry*, Vol. 98, No. 2, May 1976, pp. 593-600.

2 Zorzi, E. S., and Nelson, H. D., "Finite Element Simulation of Rotor-Bearing Systems with Internal Damping," ASME *Journal of Eng. for Power*, Vol. 99, No. 1, Jan. 1977, pp. 71-76.

3 Nelson, H. D., "A Finite Rotating Shaft Element Using Timoshenko Beam Theory," ASME *Journal of Mechanical Design*, Vol. 102, No. 4, Oct. 1980, pp. 793-803.

4 Ozguven, H. N., and Ozkan, Z. L., "Whirl Speeds and Unbalance Response of Multibearing Rotors Using Finite Element," ASME Paper 83-DET-89, Design and Production Technical Conference, Dearborn, MI, Sept. 11-14, 1983.

5 Rouch, K. E., and Kao, J. S., "A Tapered Beam Finite Element for Rotor Dynamics Analysis," *J. of Sound and Vibr.*, Vol. 66, No. 1, 1979, pp. 119-140.

6 Thomas, D. L., Wilson, J. M., and Wilson, R. R., "Timoshenko Beam Finite Elements," *J. of Sound and Vibr.*, Vol. 31, No. 3, 1973, pp. 315-330.

7 To, C. W. S., "A Linearly Tapered Beam Finite Element Incorporating Shear Deformation and Rotary Inertia for Vibration Analysis," *J. of Sound and Vibr.*, Vol. 78, No. 4, 1981, pp. 475-484.

8 DeSalvo, G. J., and Swanson, J. A., ANSYS Engineering Analysis System, Revision 4.0.


## APPENDIX

Translation Shape Function $[\psi]$, equation (6)

$$[\psi] = \begin{bmatrix} \psi_1 & 0 & 0 & \psi_2 & \psi_3 & 0 & 0 & \psi_4 & -\psi_2 & 0 & -\psi_4 & 0 \\ 0 & \psi_1 & -\psi_2 & 0 & 0 & \psi_3 & -\psi_4 & 0 & 0 & -\psi_2 & 0 & -\psi_4 \end{bmatrix}$$

where

$$\begin{aligned} \psi_1 &= 1-3\xi^2+2\xi^3 \\ \psi_2 &= l(\xi-2\xi^2+\xi^3) \\ \psi_3 &= 3\xi^2-2\xi^3 \\ \psi_4 &= l(-\xi^2+\xi^3) \end{aligned}$$

Rotational Shape Function $[\phi]$, equation (7)

$$[\phi] = \begin{bmatrix} 0 & \phi_1 & \phi_2 & 0 & 0 & -\phi_1 & \phi_3 & 0 & 0 & -\phi_4 & 0 & -\phi_4 \\ -\phi_1 & 0 & 0 & \phi_2 & \phi_1 & 0 & 0 & \phi_3 & \phi_4 & 0 & \phi_4 & 0 \end{bmatrix}$$

where

$$\begin{aligned} \phi_1 &= 6(\xi-\xi^2) \\ \phi_2 &= 1-4\xi+3\xi^2 \\ \phi_3 &= -2\xi+3\xi^2 \\ \phi_4 &= 3\xi-3\xi^2 \end{aligned}$$

Shear Deformation Shape Function $[\chi]$, equation (8)

$$[\chi] = \begin{bmatrix} 0 & 0 & 0 & 0 & 0 & 0 & 0 & 0 & \chi_1 & 0 & \chi_2 & 0 \\ 0 & 0 & 0 & 0 & 0 & 0 & 0 & 0 & 0 & \chi_1 & 0 & \chi_2 \end{bmatrix}$$

where

$$\begin{aligned} \chi_1 &= 1-\xi \\ \chi_2 &= \xi \end{aligned}$$

General Notes on Presentation of Element Matrices

The next 9 element matrices are given in array format, that is, each nonzero term will be denoted by (*ir*, *ic*), where *ir* is the row and *ic* the column in the matrix. This notation has been adopted for clarity, as each matrix term is a polynomial, except for

$[K_A]$, the axial stiffness matrix. All matrices are of size $12 \times 12$, and any term not explicitly defined is zero. Since all of the matrices are either symmetric or skew symmetric, only the lower triangular is given, with the type of symmetry given for each matrix.

Element Bending Stiffness Matrix $[K_B]$, equation (12($a$)) (sym)

$$K = EI_i/7!l^3$$

$$
\begin{aligned}
(1,1) &= K(60480 + 30240\delta_1 + 24192\delta_2 + 21168\delta_3 + 19008\delta_4) \\
(4,1) &= Kl(30240 + 10080\delta_1 + 7056\delta_2 + 6048\delta_3 + 5472\delta_4) \\
(5,1) &= (6,2) = -(2,2) = -(5,5) = -(6,6) = -(1,1) \\
(8,1) &= Kl(30240 + 20160\delta_1 + 17136\delta_2 + 15120\delta_3 + 13536\delta_4) \\
(9,1) &= -Kl(30240 + 15120\delta_1 + 12096\delta_2 + 10584\delta_3 + 9504\delta_4) \\
(11,1) &= (10,2) = (12,2) = -(9,5) = -(11,5) = -(10,6) = -(12,6) = (9,1) \\
(3,2) &= (5,4) = -(6,3) = -(4,1) \\
(7,2) &= (8,5) = -(7,6) = -(8,1) \\
(3,3) &= (4,4) = Kl^2(20160 + 5040\delta_1 + 2688\delta_2 + 2016\delta_3 + 1728\delta_4) \\
(7,3) &= (8,4) = Kl^2(10080 + 5040\delta_1 + 4368\delta_2 + 4032\delta_3 + 3744\delta_4) \\
10,3) &= Kl^2(15120 + 5040\delta_1 + 3528\delta_2 + 3024\delta_3 + 2736\delta_4) \\
(12,3) &= -(9,4) = -(11,4) = (10,3) \\
(7,7) &= (8,8) = Kl^2(20160 + 15120\delta_1 + 12768\delta_2 + 11088\delta_3 + 9792\delta_4) \\
(10,7) &= Kl^2(15120 + 10080\delta_1 + 8568\delta_2 + 7560\delta_3 + 6768\delta_4) \\
(12,7) &= -(9,8) = -(11,8) = (10,7) \\
(9,9) &= Kl^2(15120 + 7560\delta_1 + 6048\delta_2 + 5292\delta_3 + 4752\delta_4) \\
(11,9) &= (10,10) = (12,10) = (11,11) = (12,12) = (9,9)
\end{aligned}
$$

Element Shear Stiffness Matrix $[K_S]$, equation (12($b$)) (sym)

$$K = klGA_i/5!$$

$$
\begin{aligned}
(9,9) &= (10,10) = K(40 + 10\alpha_1 + 4\alpha_2) \\
(11,9) &= (12,10) = K(20 + 10\alpha_1 + 6\alpha_2) \\
(11,11) &= (12,12) = K(40 + 30\alpha_1 + 24\alpha_2)
\end{aligned}
$$

Element Axial Stiffness Matrix $[K_A]$, equation (12($c$)) (sym)

$$K = P/30l$$

$$
\begin{array}{llllllll}
(1,1) = & -(5,1) = & (2,2) = & -(6,2) = & (5,5) = & (6,6) = & 36K & \\
(4,1) = & (8,1) = & (6,3) = & (9,5) = & (11,5) = & (7,6) = & (10,6) = (12,6) = & 3Kl \\
(9,1) = & (11,1) = & (3,2) = & (7,2) = & (10,2) = & (12,2) = & (5,4) = (8,5) = & -3Kl \\
(3,3) = & (10,3) = & (4,4) = & -(9,4) = & -(11,4) = & (7,7) = & (12,7) = & 4Kl^2 \\
(8,8) = & (9,9) = & (11,9) = & (10,10) = & (11,11) = & (12,12) = & & 4Kl^2 \\
(9,8) = & (11,8) = & -(7,3) = & -(12,3) = & -(8,4) = & -(10,7) = & -(12,10) = & Kl^2
\end{array}
$$

Element Translational Mass Matrix $[M_T]$, equation (15($a$)) (sym)

$$M = \mu A_i l/9!$$

$$
\begin{aligned}
(1,1) &= (2,2) = M(134784 + 31104\alpha_1 + 10944\alpha_2) \\
(4,1) &= -(9,1) = -(3,2) = -(10,2) = Ml(19008 + 6048\alpha_1 + 2448\alpha_2) \\
(5,1) &= (6,2) = M(46656 + 23328\alpha_1 + 13248\alpha_2) \\
(11,1) &= (7,2) = (12,2) = -(8,1) = Ml(11232 + 5184\alpha_1 + 2736\alpha_2) \\
(3,3) &= Ml^2(3456 + 1296\alpha_1 + 576\alpha_2) \\
(10,3) &= (4,4) = -(9,4) = (9,9) = (10,10) = (3,3) \\
(6,3) &= -(5,4) = (9,5) = (10,6) = -Ml(11232 + 6048\alpha_1 + 3600\alpha_2) \\
(7,3) &= -Ml^2(2592 + 1296\alpha_1 + 720\alpha_2) \\
(12,3) &= (8,4) = -(11,4) = (10,7) = -(9,8) = (11,9) = (12,10) = (7,3) \\
(5,5) &= (6,6) = M(134784 + 103680\alpha_1 + 83520\alpha_2) \\
(8,5) &= -(11,5) = -(7,6) = -(12,6) = -Ml(19008 + 12960\alpha_1 + 9360\alpha_2) \\
(7,7) &= Ml^2(3456 + 2160\alpha_1 + 1440\alpha_2) \\
(12,7) &= (8,8) = -(11,8) = (11,11) = (12,12) = (7,7)
\end{aligned}
$$

Element Whirl Frame Translation Mass Matrix $[\hat{M}_T]$, equation (25) (sk-sym)

$$M = \mu A_i l/9!$$

$$
\begin{aligned}
(2,1) &= (6,5) = M(269568 + 62208\alpha_1 + 21888\alpha_2)\\
(3,1) &= (10,1) = (4,2) = -(9,2) = -Ml(38016 + 12096\alpha_1 + 4896\alpha_2)\\
(6,1) &= -(5,2) = M(93312 + 46656\alpha_1 + 26496\alpha_2)\\
(7,1) &= (12,1) = (8,2) = -(11,2) = Ml(22464 + 10368\alpha_1 + 5472\alpha_2)\\
(4,3) &= -(9,3) = -(10,4) = (10,9) = Ml^2(6912 + 2592\alpha_1 + 1152\alpha_2)\\
(5,3) &= (6,4) = -(10,5) = (9,6) = Ml(22464 + 12096\alpha_1 + 7200\alpha_2)\\
(8,3) &= (12,9) = -Ml^2(5184 + 2592\alpha_1 + 1440\alpha_2)\\
(11,3) &= Ml^2(5184 + 2592\alpha_1 + 1440\alpha_2)\\
(7,4) &= (12,4) = (9,7) = (10,8) = (11,10) = (11,3)\\
(7,5) &= (12,5) = (8,6) = -(11,6) = Ml(38016 + 25920\alpha_1 + 18720\alpha_2)\\
(8,7) &= -(11,7) = -(12,8) = (12,11) = Ml^2(6912 + 4320\alpha_1 + 2880\alpha_2)\\
(10,9) &= Ml^2(6912 + 2592\alpha_1 + 1152\alpha_2)
\end{aligned}
$$

Element Rotatory Mass Matrix $[M_R]$, equation (15($b$)) (sym)

$$M = \mu I_i/9!l$$

$$
\begin{aligned}
(1,1) &= M(435456 + 217728\delta_1 + 124416\delta_2 + 77760\delta_3 + 51840\delta_4)\\
(4,1) &= Ml(36288 + 36288\delta_1 + 25920\delta_2 + 18144\delta_3 + 12960\delta_4)\\
(5,1) &= (6,2) = -(2,2) = -(5,5) = -(6,6) = -(1,1)\\
(8,1) &= Ml(36288 - 10368\delta_2 - 12960\delta_3 - 12960\delta_4)\\
(9,1) &= -Ml(217728 + 108864\delta_1 + 62208\delta_2 + 38880\delta_3 + 25920\delta_4)\\
(11,1) &= (10,2) = (12,2) = -(9,5) = -(11,5) = -(10,6) = -(12,6) = (9,1)\\
(3,2) &= -(6,3) = (5,4) = -(4,1)\\
(7,2) &= (8,5) = -(7,6) = -(8,1)\\
(3,3) &= (4,4) = Ml^2(48684 + 12096\delta_1 + 6912\delta_2 + 4752\delta_3 + 3456\delta_4)\\
(7,3) &= (8,4) = -Ml^2(12096 + 6048\delta_1 + 5184\delta_2 + 4752\delta_3 + 4320\delta_4)\\
(10,3) &= Ml^2(18144 + 18144\delta_1 + 12960\delta_2 + 9072\delta_3 + 6480\delta_4)\\
(12,3) &= (9,4) = -(11,4) = (10,3)\\
(7,7) &= (8,8) = Ml^2(48384 + 36288\delta_1 + 31104\delta_2 + 28080\delta_3 + 25920\delta_4)\\
(10,7) &= Ml^2(18144 - 5184\delta_2 - 6480\delta_3 - 6480\delta_4)\\
(12,7) &= -(9,8) = -(11,8) = (10,7)\\
(9,9) &= Ml^2(108864 + 54432\delta_1 + 31104\delta_2 + 19440\delta_3 + 12960\delta_4)\\
(11,9) &= (10,10) = (12,10) = (11,11) = (12,12) = (9,9)
\end{aligned}
$$

Element Gyroscopic Matrix $[G]$, equation (15($c$)) (sk-sym)

$$M = \mu I_i/9!l$$

$$
\begin{aligned}
(2,1) &= M(870912 + 435456\delta_1 + 248832\delta_2 + 155520\delta_3 + 103680\delta_4)\\
(3,1) &= -Ml(72576 + 72576\delta_1 + 51840\delta_2 + 36288\delta_3 + 25920\delta_4)\\
(6,1) &= -(5,2) = -(6,5) = -(2,1)\\
(7,1) &= Ml(-72576 + 20736\delta_2 + 25920\delta_3 + 25920\delta_4)\\
(10,1) &= -Ml(435456 + 217728\delta_1 + 124416\delta_2 + 77760\delta_3 + 51840\delta_4)\\
(12,1) &= -(9,2) = -(11,2) = -(10,5) = -(12,5) = (9,6) = (11,6) = (10,1)\\
(4,2) &= (5,3) = (6,4) = (3,1)\\
(8,2) &= -(7,5) = -(8,6) = (7,1)\\
(4,3) &= Ml^2(96768 + 24192\delta_1 + 13824\delta_2 + 9504\delta_3 + 6912\delta_4)\\
(8,3) &= -(7,4) = -Ml^2(24192 + 12096\delta_1 + 10368\alpha_2 + 9504\delta_3 + 8640\delta_4)\\
(9,3) &= -Ml^2(36288 + 36288\delta_1 + 25920\delta_2 + 18144\delta_3 + 12960\delta_4)\\
(11,3) &= (10,4) = (12,4) = (9,3)\\
(8,7) &= Ml^2(96768 + 72576\delta_1 + 62208\delta_2 + 56160\delta_3 + 51840\delta_4)\\
(9,7) &= Ml^2(-36288 + 10368\delta_2 + 12960\delta_3 + 12960\delta_4)
\end{aligned}
$$

$$
\begin{aligned}
(11,7) &= (10,8) = (12,8) = (9,7)\\
(10,9) &= Ml^2(217728 + 108864\delta_1 + 62208\delta_2 + 38880\delta_3 + 25920\delta_4)\\
(12,9) &= -(11,10) = (12,11) = (10,9)
\end{aligned}
$$

Element Circulation Matrix $[K_C]$, equation (18) (sk-sym)

$$K = EI_i/7!l^3$$

$$
\begin{aligned}
(2,1) &= -K(60480 + 30240\delta_1 + 24192\delta_2 + 21168\delta_3 + 19008\delta_4)\\
(3,1) &= Kl(30240 + 10080\delta_1 + 7056\delta_2 + 6048\delta_3 + 5472\delta_4)\\
(6,1) &= -(5,2) = -(6,5) = -(2,1)\\
(7,1) &= K(30240 + 20160\delta_1 + 17136\delta_2 + 15120\delta_3 + 13536\delta_4)\\
(10,1) &= Kl(30240 + 15120\delta_1 + 12096\delta_2 + 10584\delta_3 + 9504\delta_4)\\
(12,1) &= -(9,2) = -(11,2) = -(10,5) = -(12,5) = (9,6) = (11,6) = (10,1)\\
(4,2) &= (5,3) = (6,4) = (3,1)\\
(8,2) &= -(7,5) = -(8,6) = (7,1)\\
(4,3) &= -Kl^2(20160 + 5040\delta_1 + 2688\delta_2 + 2016\delta_3 + 1728\delta_4)\\
(8,3) &= -(7,4) = -Kl^2(10080 + 5040\delta_1 + 4368\delta_2 + 4032\delta_3 + 3744\delta_4)\\
(9,3) &= Kl^2(15120 + 5040\delta_1 + 3528\delta_2 + 3024\delta_3 + 2736\delta_4)\\
(11,3) &= (10,4) = (12,4) = (9,3)\\
(8,7) &= -Kl^2(20160 + 15120\delta_1 + 12768\delta_2 + 11088\delta_3 + 9792\delta_4)\\
(9,7) &= Kl^2(15120 + 10080\delta_1 + 8568\delta_2 + 7560\delta_3 + 6768\delta_4)\\
(11,7) &= (10,8) = (12,8) = (9,7)\\
(10,9) &= -Kl^2(15120 + 7560\delta_1 + 6048\delta_2 + 5292\delta_3 + 4752\delta_4)\\
(12,9) &= -(11,10) = (12,11) = (10,9)
\end{aligned}
$$

Element Transformation Matrix $[N]$, equations (15*c*, 18, and 25)

$$[N] = \begin{bmatrix} 0 & -1 \\ 1 & 0 \end{bmatrix}$$

Element Internal Damping Matrix $[\eta]$, equation (16*a*)

$$[\eta] = \frac{1}{\sqrt{1+\eta_H{}^2}} \begin{bmatrix} (1+\eta_H) & \eta_H \\ -\eta_H & (1+\eta_H) \end{bmatrix}$$

Element Fixed to Whirl Frame Transformation Matrix $[R]$, equation (23)

For the $12\times12$ element matrices, $[R]$ is a block diagonal matrix composed of six $2\times2$ matrices each equal to $\cos\omega t[I] + \sin\omega t[N]$.

Element Unbalance Force Vectors $\{Q_C\}$ and $\{Q_S\}$, equation (20)

$$M = \Omega^2\mu A_i/7!$$

$$
\begin{aligned}
\{Q_{C1}\} &= \{Q_{S2}\} = M\epsilon_i(1764 + 420\alpha_1 + 156\alpha_2) + M\epsilon_j(756 + 336\alpha_1 + 156\alpha_2)\\
\{Q_{C2}\} &= -\{Q_{S1}\} = M\zeta_i(1764 + 420\alpha_1 + 156\alpha_2) + M\zeta_j(756 + 336\alpha_1 + 156\alpha_2)\\
\{Q_{C3}\} &= -Ml\zeta_i(252 + 84\alpha_1 + 36\alpha_2) - Ml\zeta_j(168 + 84\alpha_1 + 48\alpha_2)\\
\{Q_{C4}\} &= Ml\epsilon_i(252 + 84\alpha_1 + 36\alpha_2) + Ml\epsilon_j(168 + 84\alpha_1 + 48\alpha_2)\\
\{Q_{C5}\} &= \{Q_{S6}\} = M\epsilon_i(756 + 420\alpha_1 + 264\alpha_2) + M\epsilon_j(1764 + 1344\alpha_1 + 1080\alpha_2)\\
\{Q_{C6}\} &= -\{Q_{S5}\} = M\zeta_i(756 + 420\alpha_1 + 264\alpha_2) + M\zeta_j(1764 + 1344\alpha_1 + 1080\alpha_2)\\
\{Q_{C7}\} &= Ml\zeta_1(168 + 84\alpha_1 + 48\alpha_2) + Ml\zeta_j(252 + 168\alpha_1 + 120\alpha_2)\\
\{Q_{C8}\} &= -Ml\epsilon_i(168 + 84\alpha_1 + 48\alpha_2) - Ml\epsilon_j(252 + 168\alpha_1 + 120\alpha_2)\\
\{Q_{C9}\} &= \{Q_{S3}\} = \{Q_{S10}\} = -\{Q_{C4}\}\\
\{Q_{C10}\} &= \{Q_{S4}\} = -\{Q_{S9}\} = \{Q_{C3}\}\\
\{Q_{C11}\} &= \{Q_{S7}\} = \{Q_{S12}\} = -\{Q_{C8}\}\\
\{Q_{C12}\} &= \{Q_{S8}\} = -\{Q_{S11}\} = \{Q_{C7}\}
\end{aligned}
$$